Biosensors and Bioelectronics 201 (2022) 113969

Contents lists available at ScienceDirect

Biosensors and Bioelectronics

journal homepage: www.elsevier.com/locate/bios

Nanoglycocluster based diagnostic platform for colorimetric detection of bacteria; A comparative study analysing the effect of AuNPs size, linker length, and glycan diversity

Nitesh Priyadarshi [a,b,1], Mayur D. Ambule [c,d,1], Shimayali Kaushal [a,b], Asheesh Kumar [c], Poonam Sagar [a,b], Ajay Kumar Srivastava [c,d,**], Nitin Kumar Singhal [a,*]

[a] National Agri-Food Biotechnology Institute (NABI), Sector-81, S.A.S. Nagar, Mohali, Punjab, India
[b] Department of Biotechnology, Panjab University, Sector 25, Chandigarh, 160014, India
[c] Medicinal & Process Chemistry Division, CSIR-Central Drug Research Institute, Lucknow, 226031, India
[d] Academy of Scientific and Innovative Research, Ghaziabad, 201002, India

ARTICLE INFO

Keywords:
Nanoglycocluster
Bacteria detection
Gold nanoparticles

ABSTRACT

Nanoglycoclusters, an upcoming class of functional nanomaterial are known to drive various processes like detection, imaging, targeting proteins, cells, and bacteria. Nanoglycoclusters are a type of nanomaterial functionalized with various glycans. The array of glycan in multiple copies enhances binding affinity with proteins. Selective and sensitive bacteria/lectin interactions using nanomaterials are an emerging area of research. The measurement of different ligand receptor interactions require sophisticated analytical tools that limit the application in biosensor domain. Recently, colorimetric biosensors gained importance in the field of the biosensor for the detection of bacteria/lectins. Herein we have demonstrated that different size of gold nanoparticles (AuNPs) along with various polyethylene glycol (PEG) linkers, functionalized with synthesized monopod and tripod of mannose and galactose that have different bacteria/lectins specificity. The newly synthesized nanoglycoclusters were able to discriminate between different lectins and bacteria. The aggregation of specific nanoglycocluster upon interaction with specific bacteria/lectins revealed that mannose monopod (MM) and mannose tripod (MT) are specific to *Escherichia coli* and concanavalin A (ConA) lectin, while galactose monopod (GM) and galactose tripod (GT) are specific to *Pseudomonas aeruginosa* and Peanut agglutinin (PNA) lectin. Further, the binding events depict the affinity of tripod glycans is more with respect to its corresponding monopod glycans. Our findings explored the potential of colorimetric sensing depending upon the size of AuNPs, linker length, specificity, along with glycans density to develop user friendly diagnostic system for the detection of bacteria.

1. Introduction

In recent years, gold nanoparticles (AuNPs) based colorimetric biosensors have gained significant interest due to their sensitivity and applicability (Zhou et al., 2019; Zhu et al., 2021). AuNPs surface can be easily fabricated with different ligands that allows AuNPs to be used as colloidal sensor (Marín et al., 2014). AuNPs are red due to the surface plasmon absorption (SPR) around 520 nm and are used for different bioassays (Chen et al., 2017; Zulfiqar et al., 2020). AuNPs aggregation in colloidal solution shifts absorption peak due to the electric dipole-dipole interaction and the plasmon coupling of nanoparticles (Chen et al., 2016; Uz et al., 2016). Mirkin and co-workers have modified the AuNPs with oligonucleotides to detect the complementary DNA sequences (Georgiou et al., 2020). AuNPs have been extensively used to detect a wide range of biomolecules including carbohydrates, DNA, and proteins (Gupta et al., 2020, 2021; Kaushal et al., 2021). Lectins are carbohydrate-binding proteins that have high specificity for glycans. Glyco-AuNPs based colorimetric sensors have been used for the detection of lectins like concanavalin A (ConA) (Kaushal et al., 2019), Ricinus communis agglutinin (RCA), Cholera toxin, and virus hemagglutinin and

* Corresponding author.
** Corresponding author. National Agri-Food Biotechnology Institute (NABI), Sector-81, S.A.S. Nagar, Mohali, Punjab, India.
E-mail addresses: ajayk.srivastava@cdri.res.in (A.K. Srivastava), nitin@nabi.res.in (N.K. Singhal).
[1] These authors contributed equally.

https://doi.org/10.1016/j.bios.2022.113969
Received 9 September 2021; Received in revised form 8 December 2021; Accepted 4 January 2022
Available online 7 January 2022

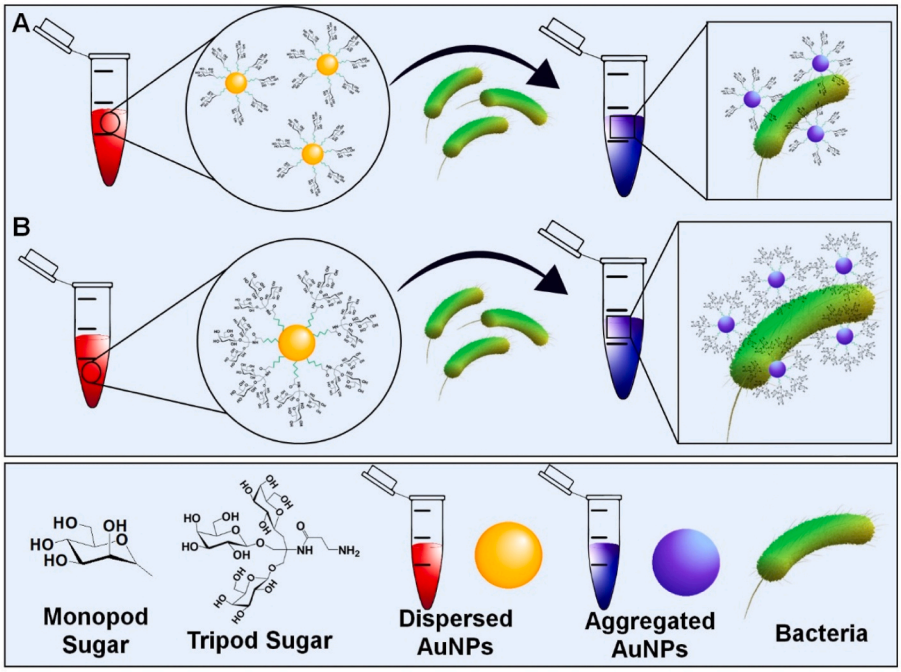

Fig. 1. Schematic representation of functionalized AuNPs with monopod sugar and tripod sugar and their aggregation in presence of target bacteria.

bacteria. Previous studies have shown the effect of size of AuNPs (Poonthiyil et al., 2015), length of linker (Schofield et al., 2008), and density of glycans (Toraskar et al., 2017) on the detection of different analytes. Carbohydrates are used extensively to study carbohydrate-carbohydrate (C–C) and carbohydrate-protein (C–P) interactions. Carbohydrates are known to offer sites for several hydrogen bonding and by exploiting this feature many research groups have synthesized various dendrimers of carbohydrates. The valency of glycans in a multivalent system is known to enhance the interaction with receptor (Timmer et al., 2016). Multivalent glycans result in enhanced binding with higher specificity and kinetic stability as compared to its corresponding monovalent glycan. Several studies have proved the role of multivalency in binding events especially in the case of carbohydrate and protein interactions (Marín et al., 2013; Online et al., 2016). By exploiting carbohydrate-protein interaction, multiple studies showed significant binding events with carbohydrate and protein. Nanotechnology has emerged as a novel technology for the detection of bacteria. AuNPs have been extensively used for detection purposes due to their good localized surface plasmon response (LSPR) (Khiavi et al., 2020; H. Wang et al., 2019; Y. Wang et al., 2019). However the current bacterial detection techniques rely on the use of expensive sophisticated instruments which require skilled manpower (Mathelié-Guinlet et al., 2019; Rubab et al., 2018). Further current detection techniques are time consuming like PCR based methods, culture based methods, and costly with low temperature storage condition for antibodies and aptamers. To make an efficient, cost-effective, and sensitive biosensor, we have synthesized multivalent glycan that have high affinity towards respective bacterial lectins. The current study critically compares the affinity of AuNPs for bacteria/lectin detection based on different sizes of AuNPs, length of Poly (ethylene glycol) 2-mercaptoethanol ether acetic acid (PEG) and diversity of glycans. Here, AuNPs were synthesized by the Turkevich method introduced in 1951(Dong et al., 2020), and two different sizes (20 nm and 40 nm) were synthesized by varying the ration of gold to citrate (Egorova et al., 2020). A very small size of AuNPs is not sensitive (Poonthiyil et al., 2015) or very long particle size is also not sensitive (Zeng et al., 2012), so we have choosen 20 and 40 nm AuNPs. Two different AuNPs were stabilized by functionalization with PEG with two different chain lengths i.e., PEG_{1000} and PEG_{5000}.

Synthesis of amine-terminated mannose monopod (MM) and galactose monopod (GM) was done by modification of the anomeric position of the mannose and galactose respectively. Mannose tripod (MT) and galactose tripod (GT) were synthesized by using click chemistry between corresponding synthesized sugar azides and alkyne. Further, the synthesized glycans were functionalized onto the surface of PEGylated AuNPs (nanoglycocluster) to design novel biosensors for specific bacterial detection (Fig. 1). The different nanoglycocluster were found to be stable at different sodium chloride (NaCl) concentration (0.01M and 0.1M NaCl), temperature condition (4 °C, 25 °C, and 37 °C), and at different pH condition (pH 3 to pH 10). The resultant nanoglycoclusters showed significant binding with respective bacteria and lectins. The tripod glycan showed higher affinity towards target bacteria/lectins as compared to the corresponding monovalent ligands. MT showed a significant increase in binding with ConA and *E. coli* with respect to its corresponding MM, which is visible through UV–visible spectrophotometry, colorimetric change, transmission electron microscopy (TEM), field emission scanning electron microscope (FE-SEM), and confocal laser scanning microscopy (CLSM). Whereas, MM and MT did not show any binding with nonspecific lectins. Similarly, GM and GT have shown binding with PNA due to their specificity with PNA and not with ConA. Further to test binding event with bacterial cell two MTCC cultures of *Escherichia coli* and *Pseudomonas aeruginosa* were allowed to interact with synthesized MM, MT, GM, and GT nanoglycoclusters. *E. coli* which contains ConA type of lectins showed significant enhancement in binding pattern with MT as compared to MM. As *Pseudomonas aeruginosa* contains PNA type of lectin, it showed an affinity for GM and GT. The affinity of these glycans has also been tested with a real sample and other standard cultures obtained from MTCC. Finally a user friendly diagnostic system has been developed for specific detection of bacteria.

2. Materials and methods

2.1. Materials

Poly (ethylene glycol) 2-mercaptoethyl ether acetic acid (PEG_{1000} and PEG_{5000}), anthrone reagent, Gold(III) chloride ($HAuCl_4$), ConA, and PNA, were purchased from Thermo fisher Scientific. 4′,6-diamidino-2-

phenylindole dihydrochloride (DAPI), 2-(N-Morpholino) ethane sulfonic acid hydrate (MES buffer) carbon coated copper grid, Tris (hydroxymethyl)aminomethane (≥99.8%), Propargyl bromide solution (80 wt% in toluene), Calcium chloride ($CaCl_2$), Potassium hydroxide (85%), Trifluoroacetic acid (99%), β-Alanine (99%), Trimethylsilyl trifluoromethane sulfonate (>99%), 2-(2-Aminoethoxy)ethanol (98%) Palladium on activated charcoal (10% Pd Basis Pd/C), β-D-Galactose pentaacetate (98%), α-D-Mannose pentaacetate (>99%), (+)-Sodium L-ascorbate (98%), Manganese chloride ($MnCl_2$), Glutaraldehyde (2%), Tannic acid, Trisodium citrate dihydrate ($Na_3C_6H_5O_7.2H_2O$), and HEPES (4- (2-hydroxyethyl)-1-piperazineethane sulfonic acid), were all purchased from Sigma-Aldrich. Sodium methoxide, Hydrogen chloride 2M in Methanol, and Sodium azide was purchased from Spectrochem. 1-[Bis(dimethylamino)methylene]-1*H*-1,2,3-triazolo[4,5-b]pyridinium3-oxid hexafluorophosphate (99%, HATU), Di-*tert*-butyl dicarbonate (99%), and Tris[(1-benzyl-1H-1,2,3-triazol-4-yl)methyl]amine (97% TBTA), were procured from TCI Ltd. Copper(II) sulfate pentahydrate (98%), HCl, NaOH, Sodium chloride (NaCl), EDC (1-ethyl-3-(3-dimethylaminopropyl) carbodiimide hydrochloride) were purchased from Avra Chemicals. Boron trifluoride diethyl etherate (99.9%), *N, N*-Diisopropylethylamine (97%, DIPEA) were purchased from Alfa Aesar. Cotton swabs and meat were purchased from nearby local shop.

2.2. Methods

2.2.1. Synthesis of glycans

Two different glycans were used as starting material namely α-D-Mannose pentaacetate and β-D-Galactose pentaacetate for the synthesis of amine-terminated monopod and tripod of the respective glycans. For the synthesis of sugar monopods anomeric position of the glycan was modified with 2-(2-azidoethoxy)ethan-1-ol to obtain ethereal linkage in monopod and for the synthesis of tripods click chemistry (Kaur et al., 2019) was performed between respective glycan azides and alkyne (SI Scheme 1, 2, and 3) (Kaur, 2019; Kaur et al., 2020).

2.2.2. Synthesis of different sizes of citrate stabilized AuNPs

Turkevich method was followed for the synthesis of citrate-capped AuNPs. 1 mL of 25 mM gold chloride was mixed with 99 mL of Milli-Q water (MQ) and kept for boiling, after which 114 mM sodium citrate was added, and the reaction was kept on boiling for the next 10 min for synthesis of 20 nm AuNPs. For the synthesis of 40 nm, AuNPs 25 mM gold chloride was mixed to 99 mL of MQ and kept for boiling, after which 57 mM sodium citrate was added, and the reaction was kept on boiling for the next 10 min for synthesis of 40 nm AuNPs. The molar ratio of sodium citrate to gold chloride was the primary factor to achieve the desired particle size (Krpetić et al., 2012). AuNPs were further functionalized with two different PEG_{1000} and PEG_{5000} separately (SI Fig. 25).

2.2.3. Carbohydrate functionalization to PEGylated AuNPs and their lectin assay

All the four different glycans namely, MM, MT, GM, and GT were functionalized on PEGylated AuNPs by using EDC chemistry. The amount of bound glycan was estimated by anthrone test. For the functionalization of glycan, respective glycans were mixed with the pellet of AuNPs and then incubated for almost 3 h at room temperature (RT) with intermittent mixing. After incubation, the pellet was washed twice with MES buffer (10,000 rpm for 45 min) and the resultant pellet was used and diluted accordingly for lectin and other bacterial aggregation assays. ConA has an affinity for mannose (Otten et al., 2016) and PNA has an affinity for galactose (Martínez-Hernández et al., 2019) and thus ConA and PNA were chosen to examine their affinity for different nanoglycoclusters. Lectins solution were prepared by dissolving in 10 nM HEPES buffer containing 0.01 mM $MnCl_2$, 0.1 mM $CaCl_2$, and 0.05 M NaCl. Different synthesized glycans were mixed with various concentrations of lectins in equal proportion (1:1) in a 96-well plate and further kept for incubation for next 30 min at RT. Post incubation the readings were recorded by UV–visible spectrophotometer.

2.2.4. Stability of different nanoglycocluster

The stability of different nanoglycocluster were tested at varying temperature (4 °C, 25 °C, and 37 °C), salt concentration (0.01M and 0.1M), and pH (3–10). For temperature study different nanoglycoclusters were stored at 4 °C, 25 °C, and 37 °C, and subsequently analysed by UV–visible spectroscopy for 0 day and at 10th day of incubation. For salt stability assay, nanoglycoclusters were diluted with different concentration of NaCl (0.01M and 0.1M) and the absorbance was measured from 350 to 800 nm using UV–visible spectroscopy for 0 h and after 24 h. For pH stability assay, nanoglycoclusters were diluted with different pH solution and UV–visible spectra were recorded at 0 h and after 24 h of incubation.

2.2.5. Bacterial detection with nanoglycoclusters

The bacterial interaction with synthesized nanoglycoclusters were analysed by TEM, FE-SEM, and CLSM. Two different microbial strains were selected i.e., *P. aeruginosa* (MTCC 1934) and *E. coli* (MTCC 443), purchased from microbial type culture collection and gene bank (MTCC). Both the cultures were stored at −20 °C which was revived by the streaking culture method on nutrient agar plates and kept for incubation at 37 °C for 16 h. Single bacterial colonies were picked from the grown culture on LB-Agar plate and were re-inoculated in nutrient broth medium and further incubated for 16–18 h at 37 °C. After incubation, the bacterial cultures were harvested by centrifugation (10,000 rpm, 10 min) and the pellet was washed twice with autoclaved phosphate buffer (PB) (1X, 0.01M) and, the cultures were serially diluted from 10^9 CFU/mL (OD-1.0) to 10^1 CFU/mL. For bacterial interaction study, different CFU/mL of bacteria were incubated with different functionalized nanoglycocluster in an equal proportion (1:1) for 30 min at RT. For TEM analysis, 10^7 CFU/mL of two different bacteria, *E. coli* and *P. aeruginosa* were pre-incubated with different nanoglycoclusters of mannose and galactose at RT for 30 min. After incubation 2 μL of the sample was coated on a TEM grid and allowed to dry for 4–5 h at RT then the sample was analysed under TEM. To test different bacteria *E. coli* MTCC 443, *E. coli* MTCC 1610 (Li et al., 2020), *Listeria monocytogenes* (MTCC 657), and *Listeria monocytogenes* (MTCC 1143) (Ceruso et al., 2020) were tested with MT and GT. Bacterial binding was also checked by FE-SEM, 10^7 CFU/mL of *E. coli* was incubated with different nanoglycocluster (MM, MT, GM, and GT) in 1:1 ratio and kept for incubation for 30 min at RT. After incubation, the cells were fixed by 2% glutaraldehyde solution for 2 h and then washed twice with PB (1X, 0.01M) and stained with tannic acid (1%) for 1 h. After incubation the sample was washed twice with PB buffer and then dehydrated serially with different concentration of ethanol (10%, 30%, 50%, 70%, 90% and 100%) with intermittent incubation of 5 min at each step. Further to check bacterial binding CLSM was used to investigate the binding of mannose and galactose probe with *P. aeruginosa* and *E. coli* respectively. Both bacteria of 10^7 CFU/mL were incubated with MM, MT, GM, and GT for 30 min at RT. The bacteria adhered with glycans functionalized nanoparticles were mixed with an organic dye DAPI (1:1000 for 10 min). Bacteria were then centrifuged (10,000 rpm for 10 min) and the pellet was resuspended in PB buffer and washed twice and then cells were fixed with 4% (w/v) paraformaldehyde (Toraskar et al., 2017). The fixed cells were casted on glass slide and analysed under CLSM.

2.2.6. Development of user friendly diagnostic system

Bacterial dilution was prepared as per standard serial dilution method for obtaining different dilution of bacteria in the range of 10^7–10^3 CFU/mL. A set of autoclaved cotton swab was dipped in the different dilutions of bacteria along with control (PB) to immobilize bacteria on cotton swabs. The immobilization of bacteria was confirmed by plating on LB agar plate. The bacteria immobilized cotton swab was dipped separately in eppendorf tubes consisting of different

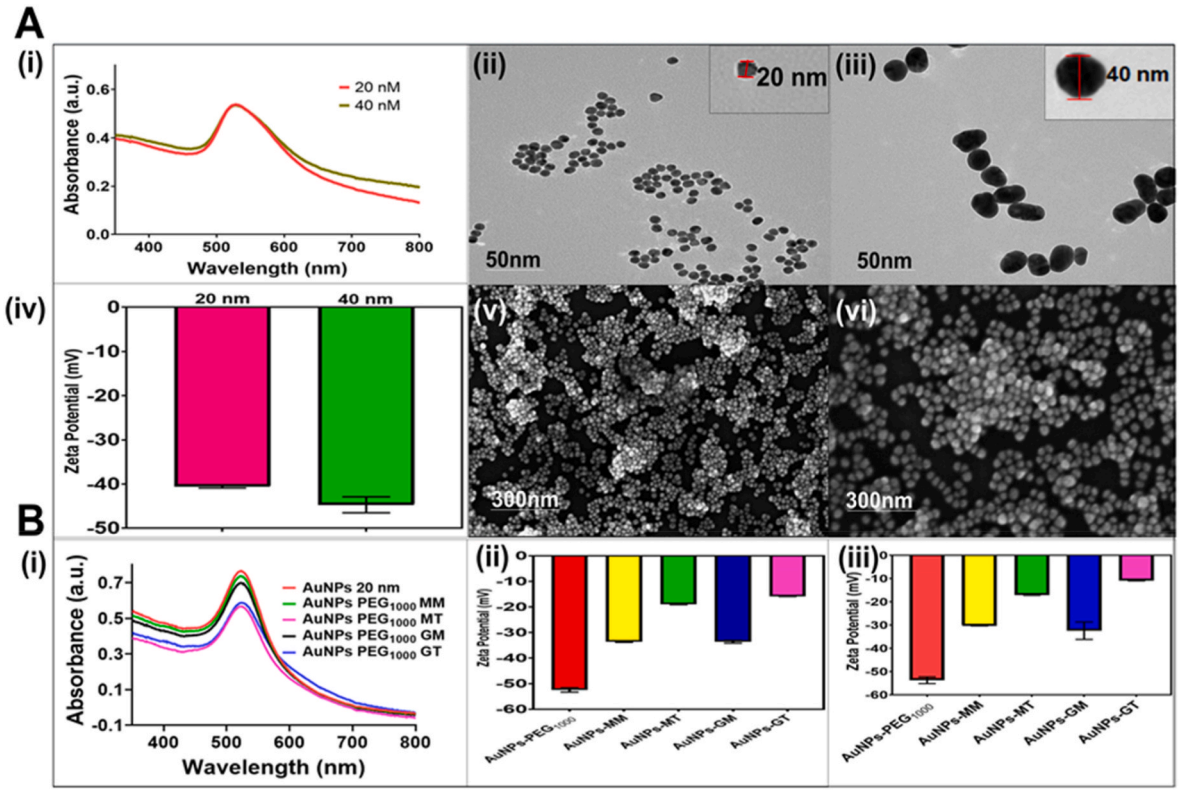

Fig. 2. Characterization of 20 nm and 40 nm AuNPs and sugar immobilization onto AuNPs. A. (i) UV–visible absorbance spectra of 20 nm AuNPs and 40 nm AuNPs. TEM image of (ii) 20 nm AuNPs (iii) 40 nm AuNPs. (iv) Zeta potential of 20 nm and 40 nm AuNPs. FE-SEM images of (v) 20 nm AuNPs (vi) 40 nm AuNPs. B. (i) UV–visible absorbance spectra of AuNPs -PEG_{1000} and different glycan functionalization. Zeta potential of (ii) 20 nm AuNPs-PEG_{1000} and different glycan functionalization (iii) 40 nm AuNPs-PEG_{1000} and different glycan functionalization.

nanoglycocluster (MT and GT) at RT for 30 min. The swabs were analysed for any colour change with respect to control (Raji et al., 2021).

2.2.7. Test on real samples

For testing of the real sample, 2 g of meat was homogenized and filtered to remove tissues debris and the filtrate was collected and diluted in a 1:10 ratio. Different CFU/mL of *E. coli* (10^8 to 10^3) were spiked in diluted meat sample and incubated with MT in 1:1 ratio at RT for 30 min for observation of colorimetric change. After incubation, the data were recorded on UV–visible spectrophotometer.

3. Result and discussion

3.1. Characterization of synthesized glycans

Glycans monopods were synthesized from previously published procedures and characterized by ^1H, ^{13}C NMR, and HRMS (Palmioli and Ferla, 2018). The synthesized glycans were characterized by ^1H NMR and ^{13}C NMR (Figs. S11-S14). Compound 1 (MM) showed a characteristic peak at δ 4.80 ppm for anomeric position H-1 as singlet (Fig. S11) and anomeric carbon peak came at δ 101.7 ppm (Fig. S12), while for compound 2 (GM) this peak came at δ 4.29 ppm for anomeric position H-1 as doublet (Fig. S13) and anomeric carbon peak came at δ 105.0 ppm (Fig. S14). Synthesized MM and GM showed HRMS peak $(M + H)^+$ at 268.1389 and 268.1383 respectively (Fig. S21 and Fig. S22). The tripod synthesized by using Click Chemistry (Henning et al., 2020) and the HRMS showed desired mass peak $(M + H)^+$ at 1186.5322 for other tripods at 1186.5315 (Fig. S23 and Fig. S24). Glycan tripods offer multiple site of interaction with receptor with respect to its monopod glycans (Budhadev et al., 2020).

3.2. Characterization of AuNPs and nanoglycocluster

AuNPs were synthesized by Turkevich method with modification for the synthesis of two different sizes of AuNPs (20 nm and 40 nm) (Shi et al., 2017). Fig. 2A illustrates the successful synthesis of 20 nm AuNPs and 40 nm AuNPs, and characterized by UV, TEM, and FE-SEM. The PEG functionalization of two AuNPs was confirmed by stability of AuNPs in presence of 0.01M NaCl with respect to bare AuNPs (Fig. S25). The stability of different nanoglycoclusters were studied at different temperature (4 °C, 25 °C, and 37 °C), (Figs. S26 and S27), salt concentration (0.01 M and 0.1M NaCl) (Fig. S28), pH (3–10) (Figs. S29 and S30), and found to be stable. The functionalization of two different PEG linker (PEG_{1000} and PEG_{5000}) and four different glycans (MM, MT, GM, and GT) onto two different AuNPs (20 nm and 40 nm) were characterized by UV–visible spectrophotometer and change in zeta potential (ζ) was recorded at each step of functionalization (Fig. 2B ii and iii). Bare $AuNPs_{20}$ nm have a zeta potential of −40.6 mV (Fig. 2A iv), which further decreased to −52.48 mV on PEG_{1000} functionalization and similarly bare $AuNPs_{40}$ nm have a zeta potential of −44.7 mV which further decreased after PEG_{1000} functionalization (ζ −55.3 mV) due to negative charge of COOH group on AuNPs. Similarly, the change in zeta potential was observed for $AuNPs_{20}$ and $AuNPs_{40}$ after PEG_{5000} functionalization (Table S1). After modification with different glycans (MM, MT, GM, and GT), zeta potential shifted towards less negative side due to the masking of COOH group as a result of amide coupling between COOH group of PEGylated AuNPs and NH_2 group of synthesized glycan (Table S1).

3.3. Quantification of synthesized glycans on AuNPs

The glycans were functionalized onto PEGylated AuNPs by EDC chemistry since PEG-AuNPs have a free carboxyl group and synthesized

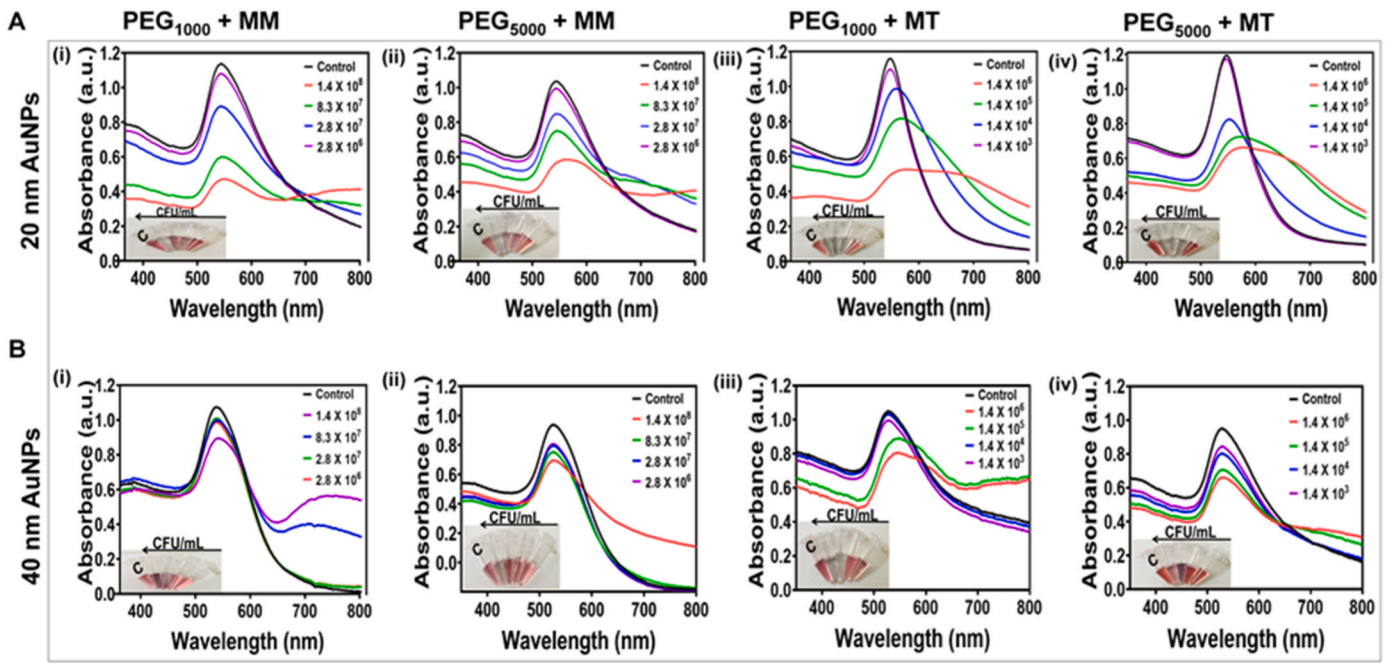

Fig. 3. Bacterial aggregation assay of *E. coli* with 20 nm and 40 nm AuNPs conjugated with two different linkers PEG_{1000} and PEG_{5000} and their subsequent conjugation with mannose monopod and mannose tripod. A. *E. coli* aggregation assay of 20 nm AuNPs functionalized with (i) MM + PEG_{1000} (ii) MM + PEG_{5000} (iii) MT + PEG_{1000} (iv) MT + PEG_{5000}. B. *E. coli* aggregation assay of 40 nm AuNPs functionalized with (i) MM + PEG_{1000} (ii) MM + PEG_{5000} (iii) MT + PEG_{1000} (iv) MT + PEG_{5000}. Abbreviations: MM (mannose monopod), MT (mannose tripod).

glycan has a free amino group, therefore amide coupling occurs between COOH group of AuNPs and NH_2 group of glycan in the presence of EDC. The amount of immobilized glycan was estimated by anthrone test and was estimated separately for each group (Fig. S31 and Table S1). The shorter linker length PEG_{1000} have less immobilized sugar due to steric hindrance between the glycans w.r.t longer length PEG_{5000} which provides degree of freedom for incorporation of more glycan on its surface.

3.4. Lectin specificity for synthesized glycans

ConA and PNA were selected to test the affinity of different synthesized nanoglycocluster and their interaction were recorded by UV–visible spectrophotometry. Different concentration of lectins were incubated with nanoglycoclusters in a ratio of 1:1 at RT for 30 min. The colorimetric change was observed in mannose with ConA (Fig. S32) due to specific ligand receptor interaction. Similarly, colorimetric change was observed for galactose with PNA (Fig. S33) due to specific ligand receptor interaction. But no significant changes were observed in PNA with mannose (Fig. S34) and ConA with galactose (Fig. S35) due to non-specificity. The lectin-nanoglycocluster interaction was also confirmed by the increase in peak at 700 nm and sharp decrease at 520 nm (Won et al., 2017). Limit of detection (LOD) of lectins for different glycan ranged from nanomolar (nM) to picomolar (pM) range as depicted in previous studies (Chen et al., 2019). The LOD of the current study in the case of MM, MT, GM and GT is 10 nM ConA, 60pM ConA, 20 nM PNA and 80pM PNA respectively for $AuNPs_{20}$- PEG_{1000} functionalized glycans (Table S1). The tripod glycan offers more site of binding with respective lectins as compared to its monopods, so tripods have lower LOD and higher sensitivity.

The shorter linker length i.e., $PEG_{1000,}$ and smaller particle diameter (20 nm) proved to be more sensitive for detection of lectin as compared to larger particle diameter (40 nm) and longer linker length i.e., PEG_{5000}. A smaller particle size have more degree of freedom to mobilise and result into faster aggregation and higher sensitivity with lower detection limits as compared to larger particle size (Zeng et al., 2012). A short chain enables formation of denser aggregates as the particles are brought closer leading to smaller interparticle distances and therefore resulting in more aggregation of AuNPs (Schofield et al., 2008). A short chain linker provides superior aggregation with lectins and bacteria displayed a lower LOD with respect to longer chain lengths. Previous studies have shown that aggregation of short chain mannose stabilized AuNPs induced by ConA (Hone et al., 2003).

3.5. Specificity of synthesized glycan for bacteria

The affinity of synthesized glycans was investigated for two different bacteria, *E. coli* and *P. aeruginosa*. Mannose has an affinity for *E. coli* due to presence of ConA lectin on the surface of *E. coli*. While galactose has an affinity for *P. aeruginosa* due to presence of PNA lectin on the surface of *P. aeruginosa*. The dissociation constant (K_d) of MM, MT, GM, and GT were 34.48 nM, 18.39 nM, 37.02 nM, and 16.15 nM respectively (Fig. S31 B) which was calculated by interaction studies with bacteria. The lower K_d value attribute to tripod glycan which shows higher binding affinity with respect to monopod glycan. To check the specificity of synthesized glycan, different CFU/mL of bacteria were incubated with nanoglycoclusters in a ratio of 1:1 at RT for 30 min. Colorimetric change, as well as a shift in UV–visible spectra, was observed in mannose conjugated AuNPs with *E. coli* (Fig. 3) and galactose with *P. aeruginosa* (Fig. S36), However there was no change in *P. aeruginosa* with mannose (Fig. S37) and *E. coli* with galactose (Fig. S38) due to absence of specific receptor-ligand interaction. LOD of bacteria for different synthesized biosensors ranged from 2.8×10^7 CFU/mL (for MM) to 1.4×10^4 CFU/mL (for MT). Previous studies have reported LOD of 1.5×10^7 CFU for monopod (Richards et al., 2014). The LOD for $AuNPs_{20}$- PEG_{1000} MM, MT, GM and GT was 2.8×10^7 CFU/mL, 1.42×10^4 CFU/mL, 2.8×10^7 CFU/mL, and 1.42×10^4 CFU/mL respectively. The tripod glycan offers more sites of binding with respective lectin present on specific bacteria compared to its corresponding monopods, so tripods displayed lower LOD with high sensitivity. The shorter linker length i.e., $PEG_{1000,}$ and smaller particle diameter (20 nm) proved to be more sensitive for detection of bacteria as compared to larger particle diameter (40 nm) and longer linker length i.

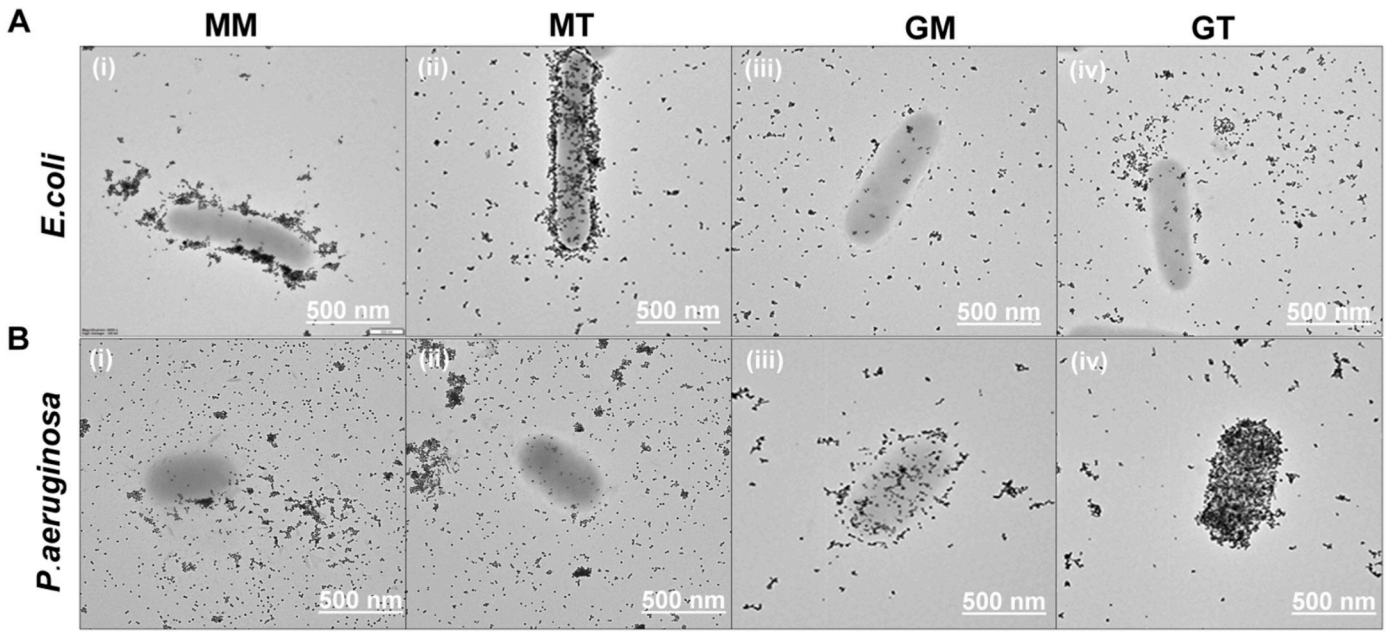

Fig. 4. TEM images of *E. coli* and *P. aeruginosa* with different MM and MT conjugated nanoparticles at 10^7 CFU/mL bacteria. A. TEM image of *E. coli* with (i) MM (ii) MT (iii) GM (iv) GT. B. TEM images of *P. aeruginosa* with (i) MM (ii) MT (iii) GM (iv) GT. Abbreviations: MM (mannose monopod), MT (mannose tripod), GM (galactose monopod), GT (galactose tripod).

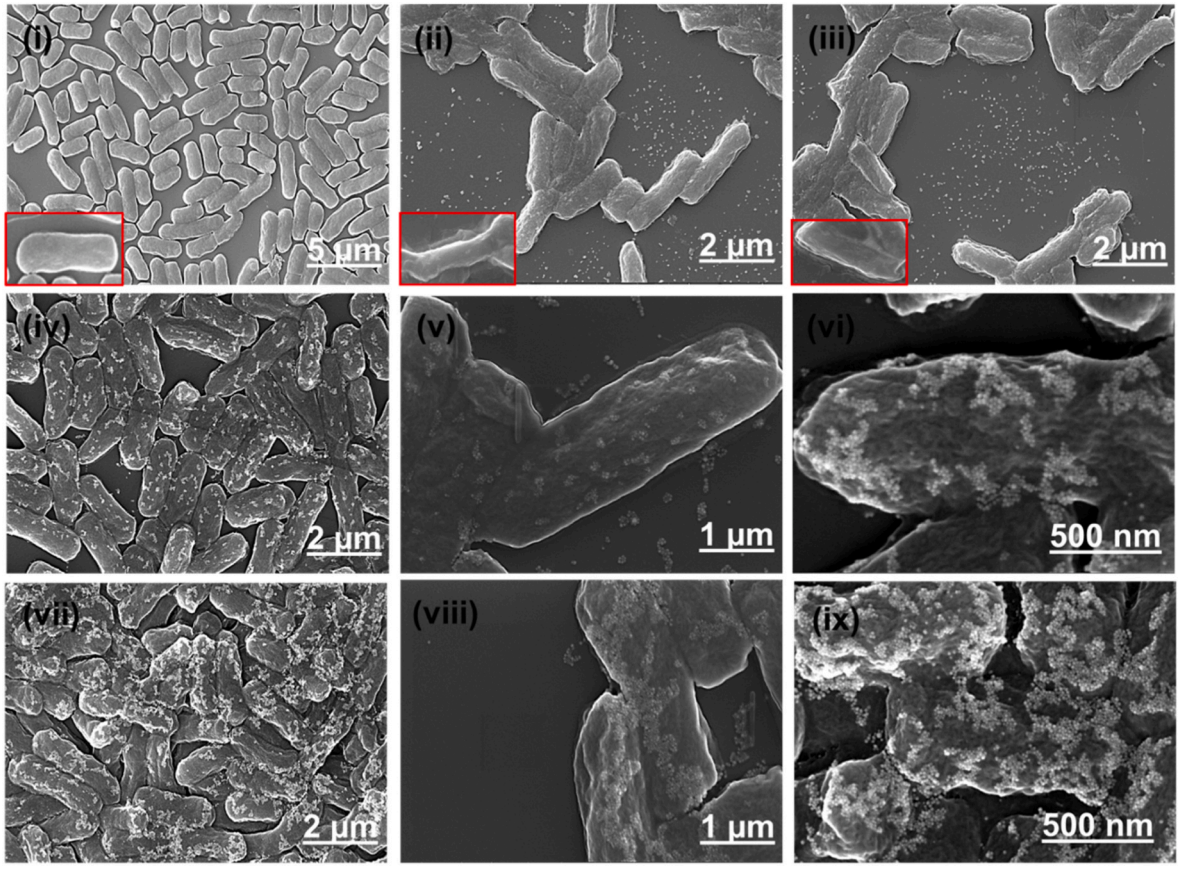

Fig. 5. FE-SEM Images of *E. coli* with different nanoglycocluster (i) Control *E. coli* (ii) *E. coli* + GM (iii) *E. coli* + GT (iv) *E. coli* + MM (v) *E. coli* + MM at 1 µm scale (vi) *E. coli* + MM at 500 nm scale (vii) *E. coli* + MT (viii) *E. coli* + MT at 1 µm scale (ix) *E. coli* + MT at 500 nm scale. Abbreviations: MM (mannose monopod), MT (mannose tripod), GM (galactose monopod), GT (galactose tripod).

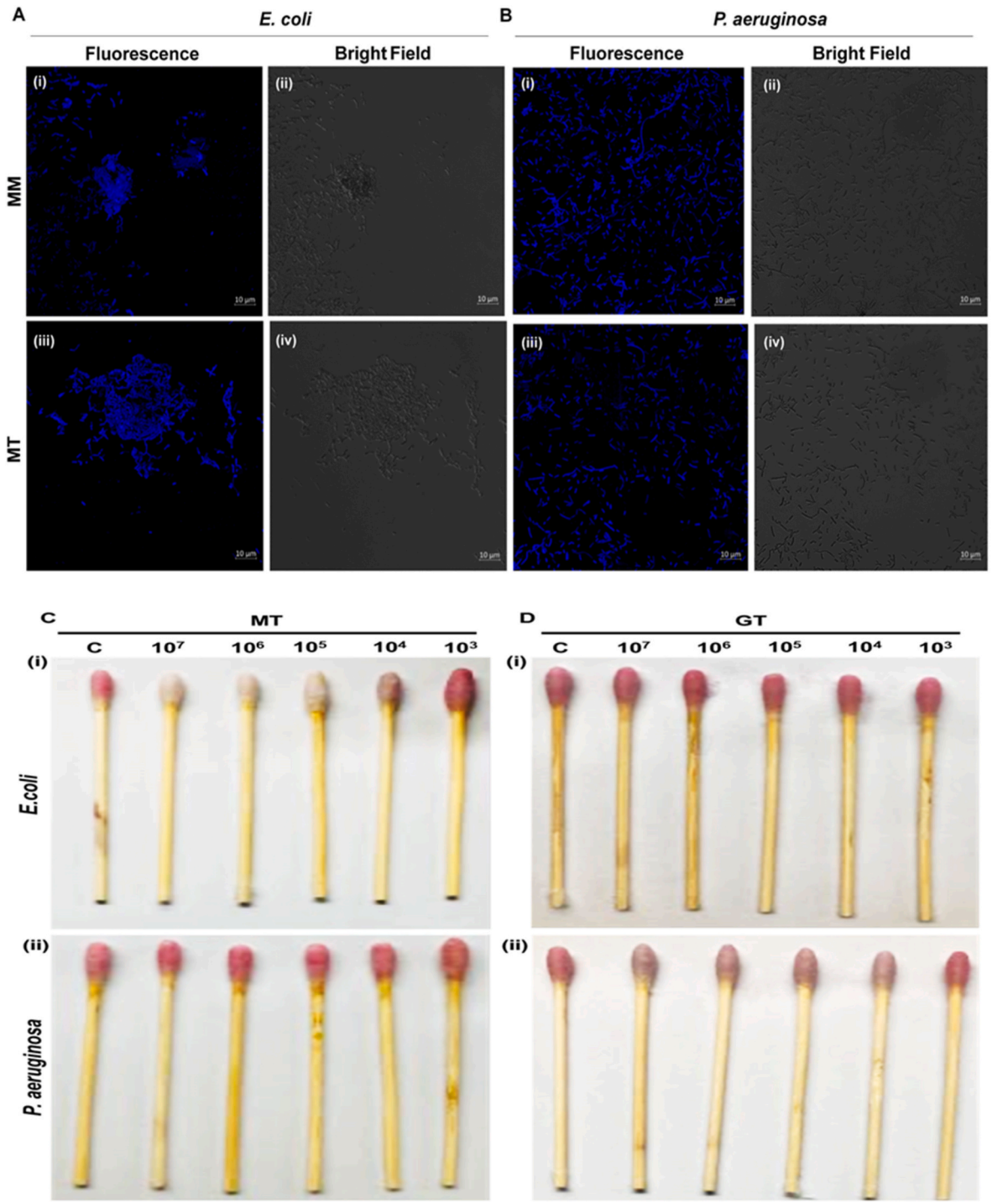

Fig. 6. A and B CLSM images of *E. coli* and *P. aeruginosa* with different MM and MT conjugated nanoparticles at 10^7 CFU/mL bacteria. A (i) & (ii) CLSM image of *E. coli* with MM. (iii) & (iv) CLSM image of *E. coli* with MT. B (i) & (ii) CLSM image of *P. aeruginosa* with MM. (iii) & (iv) CLSM image of *P. aeruginosa* with MT. C and D An easy to use diagnostic system for *E. coli* and *P. aeruginosa* with mannose tripod and galactose tripod sensor. C image of (i) *E. coli* with mannose tripod (ii) *P. aeruginosa* with mannose tripod. D image of (i) *E. coli* with galactose tripod (ii) *P. aeruginosa* with galactose tripod. Abbreviations: MM (mannose monopod), MT (mannose tripod), GT (galactose tripod).

e., PEG_{5000} (Schofield et al., 2008). So further studies were continued with $AuNPs_{20}$- PEG_{1000}.

3.6. Bacterial aggregation studies

To study the specific aggregation of glycan functionalized AuNPs, we used TEM, FE-SEM, and CLSM. TEM analysis (Fig. 4A i and ii) showed the affinity of mannose conjugated AuNPs for *E. coli* due to presence of ConA type lectin on *E. coli* surface (Yazgan et al., 2014) as the majority of mannose coated AuNPs found aggregated in close proximity of *E. coli*, whereas there is no specific aggregation of mannose conjugated AuNPs when incubated with *P. aeruginosa* (Fig. 4B i and ii) due to absence of specific receptor and vice-versa in the case of galactose conjugated AuNPs. In Fig. 4 and Fig. S39 we can observe the enhancement in the binding of AuNPs when MT is used with *E. coli* with respect to MM and the same in the case of GT along with *P. aeruginosa* (Fig. S40). Tripod

glycans offer more binding sites for respective ligands so, tripod shows higher binding pattern with respect to monopod glycans. While there was no aggregation in *P. aeruginosa* with mannose conjugated AuNPs (Fig. S41) and *E. coli* with galactose glycan (Fig. S42) due to presence of non-specific receptors on respective bacterial surface. The observed aggregation again reflects the specificity of mannose and galactose for *E. coli* and *P. aeruginosa* respectively.

In FE-SEM images of *E. coli* with different nanoglycoclusters (MM, MT, GM, and GT) (Fig. 5), the mannose functionalized AuNPs were adhered on the surface of *E. coli* (Fig. 5 iv to 5 ix) due to presence of specific receptor (ConA). Whereas the galactose functionalized AuNPs did not adhere with *E.coli* due to non-specificity (Fig. 5 ii and 5 iii). Further the MT nanoglycocluster show enhanced binding with *E.coli* surface (Fig. 5 vii to 5 ix) corresponding to MM (Fig. 5 iv to 5 vi). In CLSM (Fig. 6A) enhanced aggregation of mannose functionalized AuNPs was observed in the case of *E. coli* with respect to galactose AuNPs (Fig. S43). Further MT showed more aggregation (Fig. 6A iii) with respect to MM and not with *P. aeruginosa* (Fig. 6B). It again proves the affinity of mannose for *E. coli* cells and in the same way, the GT resulted in more aggregation with *P. aeruginosa* with respect to GM and there was no significant aggregation with *E. coli* cells (Fig. S43), due to presence of specific receptor for mannose on *E. coli* surface and galactose on *P. aeruginosa* surface.

3.7. Development of diagnostic tool for bacterial detection

The cotton swabs immobilized with bacteria *E. coli* (MTCC 443) and *P. aeruginosa* were dipped in MT and GT nanoglycocluster. The *E. coli* immobilized swab showed disappearance of red colour of AuNPs with MT in the range of 10^7 to 10^4 CFU/mL due to aggregation of MT AuNPs. However, no colour change was observed in *P. aeruginosa* immobilized swab due to non-specificity. In similar way *P. aeruginosa* immobilized swab showed change of colour in presence of GT AuNPs in the range of 10^7 to 10^4 CFU/mL due to aggregation of galactose functionalized AuNPs in the presence of PNA type of lectin present on the surface of *P. aeruginosa* and no colour change was observed in *E. coli* immobilized swab due to non-specificity (Fig. 6C and D). The visible colorimetric change was independently confirmed by four researchers for change in colour w.r.t control and nonspecific bacteria.

3.8. Specificity of different food borne bacteria and real sample testing

For studying the affinity of different bacteria, two glycans MT and GT, four food borne bacteria, *Escherichia coli* (MTCC 443), *Escherichia coli* (MTCC 1610), *Listeria monocytogenes* (MTCC 657), *Listeria monocytogenes* (MTCC 1143) were incubated in a ratio of 1:1 with functionalized AuNPs at RT. 50 μL of 10^4 CFU/mL of different bacteria were incubated with 50 μL of MT and GT AuNPs. The MT showed a spectral shift in UV–visible spectrophotometer and also colorimetric change with both the strains of *E. coli* and not with any *L. monocytogenes* (Fig. S44 A i) due to presence of specific receptor (Con A) on the surface on *E. coli*, while GT showed spectral as well as UV–visible change with both the strains of *L. monocytogenes* only and not with *E. coli* (Fig. S44 A ii) due to presence of specific receptor (PNA) (Ceruso et al., 2020) on the surface of *L. monocytogenes*. Which again proves the affinity of mannose for *E. coli* and affinity of galactose for *L. monocytogenes*. The bacterial binding with the respective glycans were also observed under TEM (Fig. S44B i and ii). In the case of a real sample, the spiked meat with *E. coli* at different dilutions (10^8 to 10^3 CFU/mL) was incubated with MT and spectral changes and colorimetric changes were observed up to 10^4 CFU/mL (Fig. S44 A iii). The binding of MT functionalized AuNPs was also observed in TEM image (Fig. S44 B iii).

3.9. Quantification of bacteria by nanoglycocluster

For quantification studies we have chosen our two best nanoglycocluster (20 nm PEG_{1000} MT and 20 nm PEG_{1000} GT). To quantify the bacteria in contaminated sample, the colour signal produced upon aggregation was converted into optical density (OD) by taking change in absorbance (ΔOD) at 520 nm with respect to control (0 CFU/mL). The change in OD (Δ OD) in contaminated sample with respect to control were plotted against different log CFU of bacteria (Sung et al., 2013). The Δ OD increases linearly as the amount of bacteria increases from 1.42×10^3 CFU/mL to 1.42×10^6 CFU/mL (Fig. S45). Both the standard curves were analysed via linear regression and the observed regression equation was $Y = 0.1802*X-0.5317$ for MT and $Y = 0.112*X-0.3195$ for GT ($R^2 = 0.98$ for MT and $R^2 = 0.97$ for GT), Where X is the cell number in log CFU. Bacteria in an unknown sample can be calculated by equation $Y = 0.1802*X-0.5317$ for MT and $Y = 0.112*X-0.3195$ for GT (Fig. S45).

4. Conclusion

In conclusion, we have synthesized four glycans and functionalized them onto two different-sized AuNPs with two distinct linkers. The lectin binding assay, bacterial aggregation assay, TEM characterization, FE-SEM characterization and CLSM analysis clearly showed the effect of nanoparticle size, linker length, and multivalency on the sensitivity towards lectins and bacteria. From the above study, we can conclude that the sensitivity of the nanoglycocluster increases with smaller nanoparticle size, shorter linker length, and multivalency of glycans. Multivalency plays a vital role in increasing the sensitivity of probes for carbohydrate-protein interaction. Overall, this study can be used to design a smart probe for in-situ rapid detection of bacteria. The user friendly diagnostic can be used to detect bacterial contamination in food samples and contaminated surfaces.

CRediT authorship contribution statement

Nitesh Priyadarshi: Mr. Nitesh Priyadarshi performed biological experiments (Detection assay, TEM, Fe-SEM, CLSM, and development of diagnostic system). **Mayur D. Ambule:** Mr. Mayur D Ambule performed the synthesis of carbohydrates derivatives and analysed the HRMS and NMR data. **Shimayali Kaushal:** Ms. Shimayali Kaushal helped in synthesis of nanoparticles and further conjugation of synthesized glycan onto it. **Asheesh Kumar:** Mr. Asheesh Kumar help in purification of synthesized carbohydrates derivatives. **Poonam Sagar:** Ms. Poonam sagar helped in designing of graphical representation of the manuscript and review of manuscript. **Ajay Kumar Srivastava :** Dr. Ajay Kumar Srivastava designed the synthetic route for carbohydrate synthesis, helped in troubleshooting and data analysis and providing funding for the work. **:** Dr Nitin Kumar Singhal conceived the idea and designed the concept, helped in troubleshooting and data analysis in writing the manuscript and providing funding for the work.

Declaration of competing interest

The authors declare that they have no known competing financial interests or personal relationships that could have appeared to influence the work reported in this paper.

Acknowledgement

The authors would like to thank the Department of Biotechnology (DBT), New Delhi; National Agri-Food Biotechnology Institute (NABI), Mohali, Indian Council of Medical Research (ICMR; Grant Number 3/1/3/JRF-2015(2)/HRD-LS/01/10137/134), New Delhi and Science and Engineering Research Board, New Delhi for their financial support (CRG_2019_004842). AMD thanks CSIR and AK thanks SERB for providing fellowships. The authors are grateful to SAIF, CSIR-CDRI, for analytical support. This manuscript bears CDRI communication number 1034300000.

Appendix A. Supplementary data

Supplementary data to this article can be found online at https://doi.org/10.1016/j.bios.2022.113969.

References

Budhadev, D., Poole, E., Nehlmeier, I., Liu, Y., Hooper, J., Kalverda, E., Akshath, U.S., Hondow, N., Turnbull, W.B., Pöhlmann, S., Guo, Y., Zhou, D., 2020. Glycan-gold nanoparticles as multifunctional probes for multivalent lectin-carbohydrate binding: implications for blocking virus infection and nanoparticle assembly. J. Am. Chem. Soc. 142, 18022–18034. https://doi.org/10.1021/jacs.0c06793.

Ceruso, M., Clement, J.A., Todd, M.J., Zhang, F., Huang, Z., Anastasio, A., Pepe, T., Liu, Y., 2020. The inhibitory effect of plant extracts on growth of the foodborne pathogen, listeria monocytogenes. Antibiotics 9, 1–13. https://doi.org/10.3390/antibiotics9060319.

Chen, J., Jackson, A.A., Rotello, V.M., Nugen, S.R., 2016. Colorimetric detection of Escherichia coli based on the enzyme-induced metallization of gold nanorods. Small 12, 2469–2475. https://doi.org/10.1002/smll.201503682.

Chen, W.J., Kandasamy, K., Chen, Y.C., 2019. Functional gold nanoparticles as sensing probes for concanavalin A and as imaging agents for cancer cells. ACS Appl. Nano Mater. 2, 3348–3357. https://doi.org/10.1021/acsanm.9b00220.

Chen, Y.-T., Su, H.-S., Hung, C.-H., Yang, P.-W., Hu, Y., Lin, T.-L., Lee, M.-T., Jeng, U.-S., 2017. X-ray reflectivity studies on the mixed Langmuir–blodgett monolayers of thiol-capped gold nanoparticles, dipalmitoylphosphatidylcholine, and sodium dodecyl sulfate. Langmuir 33, 10886–10897. https://doi.org/10.1021/acs.langmuir.7b01559.

Dong, J., Carpinone, P.L., Pyrgiotakis, G., Demokritou, P., Moudgil, B.M., 2020. Synthesis of precision gold nanoparticles using Turkevich method. Kona : Powder Sci. Technol. Japan 37, 224–232. https://doi.org/10.14356/kona.2020011.

Egorova, E.A., van Rijt, M.M.J., Sommerdijk, N., Gooris, G.S., Bouwstra, J.A., Boyle, A.L., Kros, A., 2020. One peptide for them all: gold nanoparticles of different sizes are stabilized by a common peptide amphiphile. ACS Nano 14, 5874–5886. https://doi.org/10.1021/acsnano.0c01021.

Georgiou, P.G., Baker, A.N., Richards, S., Laezza, A., Gibson, M.I., 2020. Binding With Glycosylated Nanoparticles by the Nature of the Polymer Ligand, pp. 136–145. https://doi.org/10.1039/c9tb02004g.

Gupta, R., Kumar, A., Kumar, S., Pinnaka, A.K., Singhal, N.K., 2021. Naked eye colorimetric detection of Escherichia coli using aptamer conjugated graphene oxide enclosed Gold nanoparticles. Sensor. Actuator. B Chem. 329, 129100. https://doi.org/10.1016/j.snb.2020.129100.

Gupta, R., Sagar, P., Priyadarshi, N., Kaul, S., Sandhir, R., Rishi, V., Singhal, N.K., 2020. Nanotechnology-based approaches for the detection of SARS-CoV-2. Front. Nanotechnol. 2, 1–14. https://doi.org/10.3389/fnano.2020.589832.

Henning, I., Woodward, A.W., Rance, G.A., Paul, B.T., Wildman, R.D., Irvine, D.J., Moore, J.C., 2020. A click chemistry strategy for the synthesis of efficient photoinitiators for two-photon polymerization. Adv. Funct. Mater. 30, 1–10. https://doi.org/10.1002/adfm.202006108.

Hone, D.C., Haines, A.H., Russell, D.A., 2003. Rapid, quantitative colorimetric detection of a lectin using mannose-stabilized gold nanoparticles. Langmuir 19, 7141–7144. https://doi.org/10.1021/LA034358V.

Kaur, A., et al., 2019. Multi-target-directed triazole derivatives as promising agents for the treatment of Alzheimer's disease. Bioorg. Chem. 87 https://doi.org/10.1016/j.bioorg.2019.03.058.

Kaur, Amandeep, Narang, S.S., Kaur, Anupamjeet, Mann, S., Priyadarshi, N., Goyal, B., Singhal, N.K., Goyal, D., 2019. Multifunctional mono-triazole derivatives inhibit Aβ42 aggregation and Cu2+-mediated Aβ42 aggregation and protect against aβ42-induced cytotoxicity. Chem. Res. Toxicol. 32, 1824–1839. https://doi.org/10.1021/acs.chemrestox.9b00168.

Kaur, R., Singh, R., Kumar, A., Kaur, S., Priyadarshi, N., Singhal, N.K., Singh, K., 2020. 1,2,3-Triazole β-lactam conjugates as antimicrobial agents. Heliyon 6, e04241. https://doi.org/10.1016/j.heliyon.2020.e04241.

Kaushal, S., Pinnaka, A.K., Soni, S., Singhal, N.K., 2021. Antibody assisted graphene oxide coated gold nanoparticles for rapid bacterial detection and near infrared light enhanced antibacterial activity. Sensor. Actuator. B Chem. 329, 129141. https://doi.org/10.1016/j.snb.2020.129141.

Kaushal, S., Priyadarshi, N., Pinnaka, A.K., Soni, S., Deep, A., Singhal, N.K., 2019. Glycoconjugates coated gold nanorods based novel biosensor for optical detection and photothermal ablation of food borne bacteria. Sensor. Actuator. B Chem. 289, 207–215. https://doi.org/10.1016/j.snb.2019.03.096.

Khiavi, M.A., Safary, A., Barar, J., Farzi-Khajeh, H., Barzegari, A., Mousavi, R., Somi, M. H., Omidi, Y., 2020. PEGylated gold nanoparticles-ribonuclease induced oxidative stress and apoptosis in colorectal cancer cells. Bioimpacts 10, 27–36. https://doi.org/10.15171/bi.2020.04.

Krpetić, Ž., Guerrini, L., Larmour, I.A., Reglinski, J., Faulds, K., Graham, D., 2012. Importance of nanoparticle size in colorimetric and SERS-based multimodal trace detection of Ni(II) ions with functional gold nanoparticles. Small 8, 707–714. https://doi.org/10.1002/smll.201101980.

Li, Y., Huang, T.Y., Ye, C., Chen, L., Liang, Y., Wang, K., Liu, J., 2020. Formation and control of the viable but non-culturable state of foodborne pathogen Escherichia coli O157:H7. Front. Microbiol. 11, 1–9. https://doi.org/10.3389/fmicb.2020.01202.

Marín, M.J., Rashid, A., Rejzek, M., Fairhurst, S.A., Wharton, S.A., Martin, S.R., McCauley, J.W., Wileman, T., Field, R.A., Russell, D.A., 2013. Glyconanoparticles for the plasmonic detection and discrimination between human and avian influenza virus. Org. Biomol. Chem. 11, 7101–7107. https://doi.org/10.1039/c3ob41703d.

Marín, M.J., Schofield, C.L., Field, R.A., Russell, D.A., 2014. Glyconanoparticles for colorimetric bioassays. Analyst 140, 59–70. https://doi.org/10.1039/C4AN01466A.

Martínez-Hernández, J., Seco-Rovira, V., Beltrán-Frutos, E., Ferrer, C., Serrano-Sánchez, M.I., Pastor, L.M., 2019. Lectin-binding pattern of glycoconjugates during spontaneous testicular recrudescence in Syrian hamster (Mesocricetus auratus) after exposure to short photoperiod. Andrologia 51, 1–9. https://doi.org/10.1111/and.13148.

Mathelié-Guinlet, M., Cohen-Bouhacina, T., Gammoudi, I., Martin, A., Béven, L., Delville, M.H., Grauby-Heywang, C., 2019. Silica nanoparticles-assisted electrochemical biosensor for the rapid, sensitive and specific detection of Escherichia coli. Sensor. Actuator. B Chem. 292, 314–320. https://doi.org/10.1016/j.snb.2019.03.144.

Online, V.A., Timmer, B.J.J., Abella, M., Proverbio, D., Altun, S., Ramstro, O., Aastrup, T., Vincent, S.P., 2016. ChemComm synthesis, characterization and lectin interaction. https://doi.org/10.1039/c6cc06737a, 12326-12329.

Otten, L., Vlachou, D., Richards, S.J., Gibson, M.I., 2016. Glycan heterogeneity on gold nanoparticles increases lectin discrimination capacity in label-free multiplexed bioassays. Analyst 141, 4305–4312. https://doi.org/10.1039/c6an00549g.

Palmioli, A., Ferla, B. La, 2018. Glycofunctionalization of poly(lactic-co-glycolic acid) polymers: building blocks for the generation of defined sugar-coated nanoparticles. Org. Lett. 20, 3509–3512. https://doi.org/10.1021/acs.orglett.8b01287.

Poonthiyil, V., Golovko, V.B., Fairbanks, A.J., 2015. Size-optimized galactose-capped gold nanoparticles for the colorimetric detection of heat-labile enterotoxin at nanomolar concentrations. Org. Biomol. Chem. 13, 5215–5223. https://doi.org/10.1039/c5ob00447k.

Raji, M.A., Suaifan, G., Shibl, A., Weber, K., Cialla-May, D., Popp, J., Al-Kattan, K., Zourob, M., 2021. Aptasensor for the detection of Methicillin resistant Staphylococcus aureus on contaminated surfaces. Biosens. Bioelectron. 176, 112910. https://doi.org/10.1016/j.bios.2020.112910.

Richards, S.-J., Fullam, E., Besra, G.S., Gibson, M.I., 2014. Discrimination between bacterial phenotypes using glyco-nanoparticles and the impact of polymer coating on detection readouts. J. Mater. Chem. B 2, 1490–1498. https://doi.org/10.1039/C3TB21821J.

Rubab, M., Shahbaz, H.M., Olaimat, A.N., Oh, D.H., 2018. Biosensors for rapid and sensitive detection of Staphylococcus aureus in food. Biosens. Bioelectron. 105, 49–57. https://doi.org/10.1016/j.bios.2018.01.023.

Schofield, C.L., Mukhopadhyay, B., Hardy, S.M., McDonnell, M.B., Field, R.A., Russell, D. A., 2008. Colorimetric detection of Ricinus communis Agglutinin 120 using optimally presented carbohydrate-stabilised gold nanoparticles. Analyst 133, 626–634. https://doi.org/10.1039/B715250G.

Shi, L., Buhler, E., Boué, F., Carn, F., 2017. How does the size of gold nanoparticles depend on citrate to gold ratio in Turkevich synthesis? Final answer to a debated question. J. Colloid Interface Sci. 492, 191–198. https://doi.org/10.1016/j.jcis.2016.10.065.

Sung, Y.J., Suk, H.-J., Sung, H.Y., Li, T., Poo, H., Kim, M.-G., 2013. Novel antibody/gold nanoparticle/magnetic nanoparticle nanocomposites for immunomagnetic separation and rapid colorimetric detection of Staphylococcus aureus in milk. Biosens. Bioelectron. 43, 432–439. https://doi.org/10.1016/j.bios.2012.12.052.

Timmer, B.J.J., Flos, M.A., Jørgensen, L.M., Proverbio, D., Altun, S., Ramström, O., Aastrup, T., Vincent, S.P., 2016. Spatially well-defined carbohydrate nanoplatforms: synthesis, characterization and lectin interaction study. Chem. Commun. 52, 12326–12329. https://doi.org/10.1039/C6CC06737A.

Toraskar, S., Gade, M., Sangabathuni, S., Thulasiram, H.V., 2017. Exploring the influence of shapes and heterogeneity of glyco-gold nanoparticles on bacterial binding for preventing infections. Chem. Med. Chem. 1–10. https://doi.org/10.1002/cmdc.201700218.

Uz, M., Bulmus, V., Altinkaya, S.A., 2016. Effect of PEG grafting density and hydrodynamic volume on gold nanoparticle–cell interactions: an investigation on cell cycle, apoptosis, and DNA damage. Langmuir 32, 5997–6009. https://doi.org/10.1021/ACS.LANGMUIR.6B01289.

Wang, H., Ouyang, W., Zhang, X., Xue, J., Lou, X., Fan, R., Zhao, X., Shan, L., Jiang, T., 2019. Bacteria-induced aggregation of bioorthogonal gold nanoparticles for SERS imaging and enhanced photothermal ablation of Gram-positive bacteria. J. Mater. Chem. B 7, 4630–4637. https://doi.org/10.1039/c9tb00845d.

Wang, Y., Jin, Y., Chen, W., Wang, J., Chen, H., Sun, L., Li, X., Ji, J., Yu, Q., Shen, L., Wang, B., 2019. Construction of nanomaterials with targeting phototherapy properties to inhibit resistant bacteria and biofilm infections. Chem. Eng. J. 358, 74–90. https://doi.org/10.1016/j.cej.2018.10.002.

Won, S., Richards, S.J., Walker, M., Gibson, M.I., 2017. Externally controllable glycan presentation on nanoparticle surfaces to modulate lectin recognition. Nanoscale Horiz. 2, 106–109. https://doi.org/10.1039/c6nh00202a.

Yazgan, I., Noah, N.M., Toure, O., Zhang, S., Sadik, O.A., 2014. Biosensor for selective detection of E. coli in spinach using the strong affinity of derivatized mannose with fimbrial lectin. Biosens. Bioelectron. 61, 266–273. https://doi.org/10.1016/j.bios.2014.05.008.

Zeng, S., Cai, M., Liang, H., Hao, J., 2012. Size-dependent colorimetric visual detection of melamine in milk at 10 ppb level by citrate-stabilized Au nanoparticles. Anal. Methods 4, 2499–2505. https://doi.org/10.1039/C2AY25319D.

Zhou, Y., Ma, M., He, H., Cai, Z., Gao, N., He, C., Chang, G., Wang, X., He, Y., 2019. Highly sensitive nitrite sensor based on AuNPs/RGO nanocomposites modified

graphene electrochemical transistors. Biosens. Bioelectron. 146, 111751. https://doi.org/10.1016/j.bios.2019.111751.
Zhu, A., Ali, S., Xu, Y., Ouyang, Q., Chen, Q., 2021. A SERS aptasensor based on AuNPs functionalized PDMS film for selective and sensitive detection of Staphylococcus aureus. Biosens. Bioelectron. 172, 112806. https://doi.org/10.1016/j.bios.2020.112806.
Zulfiqar, A., Temerov, F., Saarinen, J.J., 2020. Multilayer TiO2 inverse opal with gold nanoparticles for enhanced photocatalytic activity. ACS Omega 5, 11595–11604. https://doi.org/10.1021/acsomega.0c00833.

Nitesh Priyadarshi has received his MSc. Degree from Pondicherry University, Pondicherry. He is currently a PhD student at National Agri Food Biotechnology Institute, Mohali. His research interests include the synthesis of multivalent carbohydrates and the development of biosensors for the detection of food-borne bacteria.

Mayur D. Ambule has received his M.Sc. Degree from the University of Pune, Pune. He is currently PhD student at CSIR-Central Drug Research Institute, Lucknow, India. His research interest includes the total synthesis of alkaloid mimics by utilizing smart post-IMCR modifications and method development for API synthesis.

Shimayali Kaushal has received her PhD Degree from Panjab University, Chandigarh. Her research interests include the development of biosensors for the detection and killing of food-borne bacteria.

Poonam Sagar received her M.Sc. degree from Banaras Hindu University, Varanasi. She is currently a PhD student at National Agri Food Biotechnology Institute, Mohali. Her research interests include the development of oral supplements for iron deficiency anemia.

Asheesh Kumar has received his M.Sc. Degree from the CSJM University, Kanpur. He is currently a Project-SRF student at CSIR-Central Drug Research Institute, Lucknow, India. His research interest includes the Asymmetric synthesis, development of novel synthetic routes for anti-tubercular drug discovery.

Ajay Kumar Srivastava received his PhD degree from CSIR-Central Drug Research Institute, Lucknow, India. Thereafter, he worked as a postdoctoral research fellow at Seoul National University, South Korea. He started his independent research career in 2011 at CSIR-Indian Institute of Chemical Technology, Hyderabad, India. Since then, he is involved in various drug discovery and process development projects. In the year 2017, he moved to CSIR-Central Drug Research Institute, Lucknow, India. His research focus involves the development of multicomponent reactions, atom-economic non-catalytic processes, green chemistry, medicinal chemistry and total synthesis.

Nitin Kumar Singhal received his PhD degree from Indian Institute of Technology Bombay, Mumbai, Department of Chemistry. He received Brain Pool Post-doctoral research fellowship and worked as a postdoctoral fellow from May 2009–Jan 2012 in Seoul National University. He is currently working as Scientist E in National Agri Food Biotechnology Institute, Mohali and his research interest covers Nanobioscience, Organic Chemistry and Metabolic Syndromes. He is also a recipient of Fulbright-Nehru Academic and professional Excellence Fellowship.